

## 7.2 Smale horseshoe and its applications

### 7.2.1 Geometrical Smale horseshoe

Let  $S \subset \mathbb{R}^2$  be the unit square in the plane (see Figure 7.9).

$$S = \{(\xi, \eta)^T \in \mathbb{R}^2 : 0 \leq \xi \leq 1, 0 \leq \eta \leq 1\}.$$

**Definition 7.26** The graph  $\Gamma_u \subset S$  of a scalar continuous function  $\eta = u(\xi)$  satisfying

(i)  $0 \leq u(\xi) \leq 1$  for  $0 \leq \xi \leq 1$ ,

(ii)  $|u(\xi_1) - u(\xi_2)| \leq \mu|\xi_1 - \xi_2|$  for  $0 \leq \xi_1 \leq \xi_2 \leq 1$ , where  $0 < \mu < 1$ ,

is called a  $\mu$ -**horizontal curve** in  $S$ .

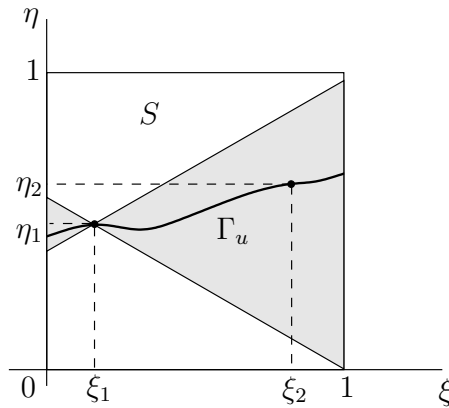


Figure 7.9: A horizontal curve.

**Definition 7.27** A graph  $\Gamma_v \subset S$  of a scalar continuous function  $\xi = v(\eta)$  satisfying:

(i)  $0 \leq v(\eta) \leq 1$  for  $0 \leq \eta \leq 1$ ;

(ii)  $|v(\eta_1) - v(\eta_2)| \leq \mu|\eta_1 - \eta_2|$  for  $0 \leq \eta_1 \leq \eta_2 \leq 1$ , where  $0 < \mu < 1$ ,

is called a  $\mu$ -**vertical curve** in  $S$ .

**Lemma 7.28** A  $\mu$ -horizontal curve  $\Gamma_h \subset S$  and a  $\mu$ -vertical curve  $\Gamma_v \subset S$  intersect in precisely one point.

**Proof:** A point of intersection  $(\xi, \eta)$  corresponds to a zero  $\xi$  of  $\xi - v(u(\xi))$  via  $\eta = u(\xi)$ . From the above definitions, one has for  $0 \leq \xi_1 < \xi_2 \leq 1$ :

$$|v(u(\xi_1)) - v(u(\xi_2))| \leq \mu|u(\xi_1) - u(\xi_2)| \leq \mu^2|\xi_1 - \xi_2|$$

with  $\mu^2 < 1$ . Hence, the function  $\psi(\xi) = \xi - v(u(\xi))$  is strictly monotonically increasing. Since  $\psi(0) < 0$  and  $\psi(1) > 0$ , it has precisely one zero.  $\square$

For  $x = (\xi, \eta)^T$ , denote

$$\|x\|_1 = |\xi| + |\eta|.$$

Introduce

$$\|u\| = \max_{0 \leq \xi \leq 1} |u(\xi)|, \quad \|v\| = \max_{0 \leq \eta \leq 1} |v(\eta)|.$$

**Lemma 7.29** *Let  $\eta = u_{1,2}(\xi)$  define two  $\mu$ -horizontal curves while  $\xi = v_{1,2}(\eta)$  define two  $\mu$ -vertical curves. Denote by  $x_{1,2} = (\xi_{1,2}, \eta_{1,2})^T$  the intersection points of the corresponding horizontal and vertical curves. Then*

$$\|x_2 - x_1\|_1 \leq \frac{1}{1 - \mu} (\|u_2 - u_1\| + \|v_2 - v_1\|). \quad (7.16)$$

**Proof:** Since  $\xi_i = v_i(\eta_i)$ , one has

$$|\xi_2 - \xi_1| \leq |v_2(\eta_2) - v_1(\eta_2)| + |v_1(\eta_2) - v_1(\eta_1)| \leq \|v_2 - v_1\| + \mu|\eta_2 - \eta_1|.$$

Similarly,

$$|\eta_2 - \eta_1| \leq \|u_2 - u_1\| + \mu|\xi_2 - \xi_1|.$$

Addition of these inequalities gives (7.16), since  $0 < \mu < 1$ .  $\square$

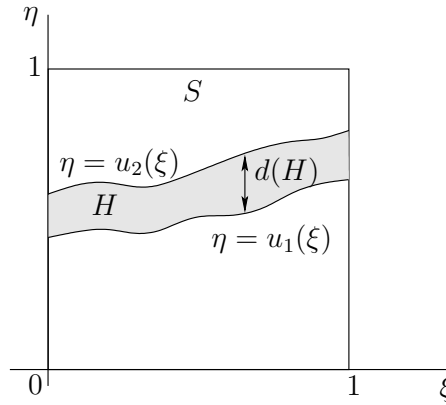


Figure 7.10: A horizontal strip.

**Definition 7.30** *The closed set  $H \subset S$  bounded by two nonintersecting  $\mu$ -horizontal curves  $\Gamma_{u_1, u_2} \subset S$  and two vertical line segments (see Figure 7.2.1) is called a  $\mu$ -horizontal strip. The number*

$$d(H) = \|u_1 - u_2\|$$

*is called the diameter of  $H$ .*

The following lemma is obvious.

**Lemma 7.31** *If*

$$H^{(1)} \supset H^{(2)} \supset H^{(3)} \dots$$

*is a sequence of nested  $\mu$ -horizontal strips  $H^{(k)}$ ,  $k = 1, 2, \dots, \infty$ , and  $d(H^{(k)}) \rightarrow 0$  as  $k \rightarrow \infty$  then*

$$\bigcap_{k=1}^{\infty} H^{(k)}$$

*is a  $\mu$ -horizontal curve.  $\square$*

One can analogously define a  $\mu$ -vertical strip  $V$  and its diameter  $d(V)$ . A lemma similar to Lemma 7.31 applies to nested vertical strips.

**Definition 7.32** Suppose that  $H_{1,2} \subset S$  are two disjoint  $\mu$ -horizontal strips, while  $V_{1,2} \subset S$  are two disjoint vertical strips. A homeomorphism  $f : \mathbb{R}^2 \rightarrow \mathbb{R}^2$  is called a **horseshoe map** if it has the following properties:

(H.1)  $f(H_i) = V_i$ ,  $i = 1, 2$ , and the horizontal/vertical boundaries of  $H_i$  are mapped onto the horizontal/vertical boundaries of  $V_i$ , respectively.

(H.2)  $H_{ij} = H_i \cap f^{-1}(H_j)$  is a  $\mu$ -horizontal strip and  $V_{ij} = f(V_i) \cap V_j$  is a  $\mu$ -vertical strip, and for some  $\nu$  with  $0 < \nu < 1$

$$d(H_{ij}) \leq \nu d(H_k), \quad d(V_{ij}) \leq \nu d(V_k),$$

for  $i, j, k = 1, 2$ .

**Example 7.33 (Geometrical Smale Horseshoe)**

Define a homeomorphism  $f : \mathbb{R}^2 \rightarrow \mathbb{R}^2$  by the geometrical construction in Figure 7.11. It acts on the unit square  $S = ABCD$  as a strong contraction in the horizontal direction, followed by a strong expansion in the vertical direction, folding, and placing back over  $ABCD$ . Suppose that

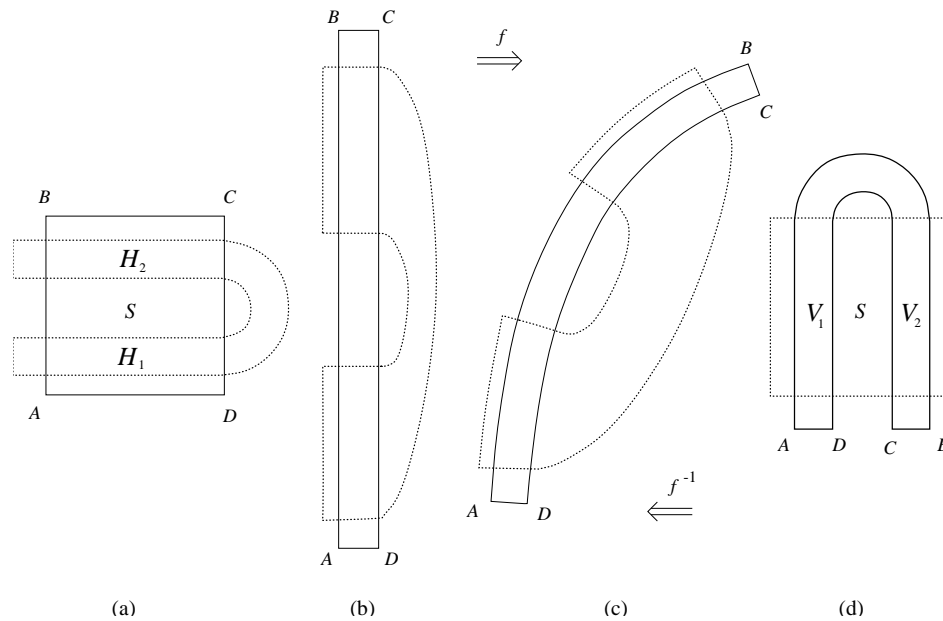


Figure 7.11: Construction of the horseshoe map:  $f(H_i) = V_i$ ,  $i = 1, 2$ .

$$f(S) \cap S = V_1 \cup V_2,$$

where  $V_{1,2}$  are two disjoint vertical rectangles. Introduce also two disjoint horizontal rectangles  $H_i$  such that

$$H_1 \cup H_2 = (f^{-1}(S)) \cap S,$$

and number them to have

$$f(H_i) = V_i, \quad i = 1, 2.$$

Assume that the map  $f : H_i \rightarrow V_i$  is linear for  $i = 1, 2$ . Then,  $f$  possesses the

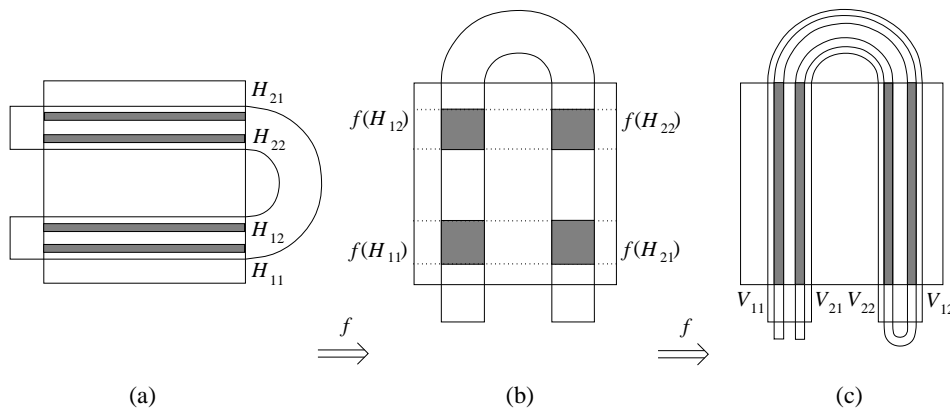


Figure 7.12:  $V_{ij} = f^2(H_{ij})$ ,  $i, j = 1, 2$ .

properties (H.1) and (H.2) of a horseshoe map. (The second should become evident while carefully looking at Figure 7.12.)  $\diamond$

The following considerations will resemble those in Section 7.1.2 concerning the ‘Big Tent Map’ (7.8). For a general horseshoe map  $f$ , define an invariant set  $\Lambda \subset S$ :

$$\Lambda = \{x \in S : f^k(x) \in S, \text{ for all } k \in \mathbb{Z}\}$$

and recall that  $\Omega_2$  denotes the set of all bi-infinite sequences of two numbers  $\{1, 2\}$  with the distinguished zero position and the distance

$$\rho(\omega, \theta) = \sum_{k \in \mathbb{Z}} \frac{|\omega_k - \theta_k|}{2^{|k|}}. \tag{7.17}$$

**Lemma 7.34** *The map  $h : \Lambda \rightarrow \Omega_2$  defined by  $h(x) = \omega$  with*

$$\omega_k = \begin{cases} 1 & \text{if } f^k(x) \in H_1, \\ 2 & \text{if } f^k(x) \in H_2, \end{cases}$$

*for  $k \in \mathbb{Z}$ , is a homeomorphism.*

**Proof:** Clearly, the formula defines a map  $h : \Lambda \rightarrow \Omega_2$ , which assigns a sequence to each point of the invariant set.

To verify that this map is invertible, take a sequence  $\omega \in \Omega_2$ , fix  $m > 0$ , and consider the set  $R_m(\omega)$  of all points  $x \in S$ , not necessarily belonging to  $\Lambda$ , such that

$$f^k(x) \in H_{\omega_k},$$

for  $-m \leq k \leq m - 1$ . For example, if  $m = 1$ , the set  $R_1$  is one of the four intersections  $V_j \cap H_k$ . In general,  $R_m$  belongs to the intersection of a vertical and a horizontal strip. The property (H.2) implies that these strips are nested and that their diameters tend to zero as  $m \rightarrow +\infty$ . By Lemma 7.31, they approach in the limit a vertical and a horizontal curve, respectively. According to Lemma 7.28, such curves intersect at a single point  $x$  with  $h(x) = \omega$ . Thus,  $h : \Lambda \rightarrow \Omega_2$  is a one-to-one map and hence  $h^{-1}$  exists.

To prove that  $h^{-1}$  is continuous, consider two sequences  $\omega, \theta \in \Lambda$ , which are close to each other (with respect to the distance (7.17)). This means that they have long coinciding central blocks:

$$\omega_k = \theta_k, \quad -m \leq k \leq m - 1.$$

This implies that

$$x, y \in R_m(\omega) = R_m(\theta),$$

where  $x = h^{-1}(\omega)$ ,  $y = h^{-1}(\theta)$ . Therefore,  $\|y - x\|_1 \rightarrow 0$  as  $m \rightarrow \infty$ , i.e.  $y \rightarrow x$  in  $\mathbb{R}^2$  as  $\rho(\omega, \theta) \rightarrow 0$ .

Thus,  $h^{-1} : \Omega_2 \rightarrow \Lambda$  is a continuous one-to-one map from the compact space  $\Omega_2$  to the compact set  $\Lambda \subset \mathbb{R}^2$ . Therefore, its inverse  $h : \Lambda \rightarrow \Omega_2$  is also continuous.  $\square$

Let  $\sigma : \Omega_2 \rightarrow \Omega_2$  be the *shift map*:

$$\theta = \sigma(\omega), \quad \theta_k = \omega_{k+1}.$$

The following is a direct implication of the definition of  $h$ .

**Lemma 7.35**  $h(f(x)) = \sigma(h(x))$  for all  $x \in \Lambda$ .  $\square$

From the basic properties of the discrete-time dynamical system  $\{\mathbb{Z}, \Omega_2, \sigma^k\}$  established in Theorem 7.14 it now immediately follows:

**Theorem 7.36 (Smale, 1963)** *Any horseshoe map  $f$  has a closed invariant set  $\Lambda$  that contains a countable set of periodic orbits of arbitrarily long period, and an uncountable set of nonperiodic orbits, among which there is an orbit passing arbitrarily close to any point of  $\Lambda$ .*

Our next aim is to replace (H.2) of Definition 7.32 by a more easily verifiable sufficient condition. For a constant  $0 < \mu < 1$  define two *cones*:

$$K^+ = \{(\xi, \eta)^T \in \mathbb{R}^2 : |\xi| \leq \mu|\eta|\}, \quad K^- = \{(\xi, \eta)^T \in \mathbb{R}^2 : |\eta| \leq \mu|\xi|\}.$$

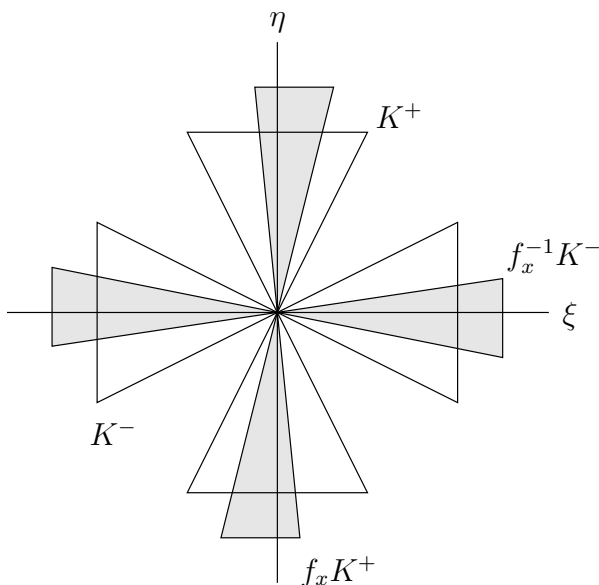
**Definition 7.37** A diffeomorphism  $f : \mathbb{R}^2 \rightarrow \mathbb{R}^2$  satisfies the  $\mu$ -*cone condition* on  $D \subset S$ , if

(i) for all  $p \in D$ ,

$$[f_x(p)]K^+ \subset K^+, \quad [f_x(p)]^{-1}K^- \subset K^-;$$

(ii) for all  $p \in D$  and

$$\begin{pmatrix} \xi_2 \\ \eta_2 \end{pmatrix} = [f_x(p)] \begin{pmatrix} \xi_1 \\ \eta_1 \end{pmatrix},$$


 Figure 7.13: The  $\mu$ -cone condition.

the following inequalities are valid:

$$|\eta_1| \leq \mu|\eta_2|, \quad \begin{pmatrix} \xi_1 \\ \eta_1 \end{pmatrix} \in K^+,$$

and

$$|\xi_2| \geq \mu|\xi_1|, \quad \begin{pmatrix} \xi_1 \\ \eta_1 \end{pmatrix} \in K^-$$

(see Figure 7.13).

**Theorem 7.38** Let  $0 < \mu < \frac{1}{2}$ , let  $V_{1,2} \subset S$  be two disjoint  $\mu$ -vertical strips with smooth vertical boundaries, and let  $H_{1,2} \subset S$  be two disjoint  $\mu$ -horizontal strips with smooth horizontal boundaries. Suppose that a map  $f : \mathbb{R}^2 \rightarrow \mathbb{R}^2$  is a diffeomorphism of the domain

$$D = H_1 \cup H_2$$

onto its image  $f(D)$  with the following properties:

(H.1)  $f(H_i) = V_i$ ,  $i = 1, 2$ , such that the horizontal/vertical boundaries of  $H_i$  are mapped onto the horizontal/vertical boundaries of  $V_i$ , respectively;

(H.3)  $f$  satisfies the  $\mu$ -cone condition in  $D$ ;

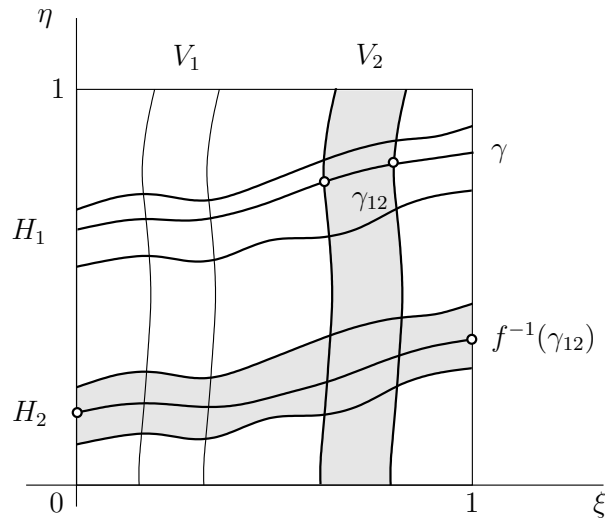
Then the map  $f$  is a horseshoe map with  $\nu = \mu(1 - \mu)^{-1}$ .

**Proof:** It suffices to show that the conditions (H.1) and (H.3) of the Theorem imply condition (H.2) from Definition 7.32.

Let  $\gamma$  be a smooth  $\mu$ -horizontal curve in a horizontal strip  $H_i$  with  $i = 1$  or  $2$ . (In Figure 7.14,  $i = 1$ .) As such it intersects every vertical curve and, in particular, the boundaries of  $V_j$ ,  $j = 1, 2$  (in Figure 7.14, we shade  $j = 2$ ). Thus  $\gamma_{ij} = \gamma \cap V_j$  connects the vertical boundaries of  $V_j$ , so necessarily  $f^{-1}(\gamma_{ij})$  connects the vertical boundaries of  $f^{-1}(V_j) = H_j$ , i.e. the vertical sides of  $S$ .

We want to show that  $f^{-1}(\gamma_{ij})$  is a horizontal curve. For this purposes we observe that  $\gamma$  is horizontal and is given, say, by a smooth function  $\eta = u(\xi)$ , satisfying

$$|u(\xi_1) - u(\xi_2)| \leq \mu|\xi_1 - \xi_2|.$$

Figure 7.14:  $f^{-1}(\gamma_{12})$  is a horizontal curve.

Since  $[f_x]^{-1}$  maps  $K^-$  into  $K^-$ , it follows by application of the Intermediate Value Theorem that for any two points  $(\xi_1, \eta_1), (\xi_2, \eta_2) \in f^{-1}(\gamma_{ij})$  one has

$$|\eta_1 - \eta_2| \leq \mu |\xi_1 - \xi_2|.$$

This shows that  $f^{-1}(\gamma_{ij})$  is the graph of a function  $\eta = w(\xi)$  defined for  $\xi \in [0, 1]$  and satisfying

$$|w(\xi_1) - w(\xi_2)| \leq \mu |\xi_1 - \xi_2|.$$

We apply this observation to the horizontal boundaries of  $H_i$  and conclude that  $f^{-1}(H_i) \cap H_j$  is a  $\mu$ -horizontal strip. Similar arguments prove that  $f(V_i) \cap V_j$ ,  $i, j = 1, 2$ , are  $\mu$ -vertical strips.

To verify the statement about the diameters, take two points  $p_{1,2} = (\xi, \eta_{1,2})$  with the same  $\xi$ -coordinate on the horizontal boundaries of  $f^{-1}(H_i) \cap H_j$ , such that

$$d(f^{-1}(H_i) \cap H_j) = |\eta_1 - \eta_2|.$$

The line segment

$$p(t) = (1-t)p_1 + tp_2, \quad t \in [0, 1],$$

is parallel to the  $\eta$ -axis and hence  $\dot{p} \in K^+$ . Therefore, its image curve,

$$z(t) = f(p(t))$$

has its tangent vector  $\dot{z} = [f_x(p(t))]\dot{p} \in K^+$  by the assumption (H.3) of the theorem. This shows that  $z(0)$  and  $z(1)$  lie on a vertical curve, for example, the one obtained by extending  $z(t)$  by two vertical segments. Thus, the points lie on a single vertical curve and two horizontal curves at a distance  $d(H_i)$ . From Lemma 7.29 follows that

$$\|z(0) - z(1)\|_1 \leq (1 - \mu)^{-1} d(H_i).$$

Writing  $z(t) = (\xi(t), \eta(t))^T$ , we have by (H.3) that

$$|\dot{\eta}| \geq \frac{1}{\mu} \|\dot{p}\|_1 > 0$$

hence  $\dot{\eta}$  does not change sign and

$$|\eta_1 - \eta_2| = \|p(0) - p(1)\|_1 = \int_0^1 \|\dot{p}\|_1 dt$$

$$\begin{aligned} &\leq \mu \int_0^1 |\dot{\eta}| dt = \mu |\eta(1) - \eta(0)| \\ &\leq \mu \|z(1) - z(0)\|_1 \leq \mu(1 - \mu)^{-1} d(H_i), \end{aligned}$$

which verifies  $\nu = \mu(1 - \mu)^{-1}$ .  $\square$

The Theorem implies, that

$$\Lambda = \{x \in D : f^k(x) \in D \text{ for all } k \in \mathbb{Z}\}$$

is an invariant set for  $f$ . Moreover, the restriction of  $f$  to  $\Lambda$  is topologically conjugated to the shift  $\sigma$  on the set  $\Omega_2$ .

## 7.2.2 Shilnikov homoclinic orbits to a saddle-focus

Smale Horseshoes appear frequently in Poincaré maps related to homoclinic bifurcations of ODEs.

**Theorem 7.39 (Shilnikov, 1965)** Consider a smooth three-dimensional system

$$\dot{x} = f(x, \alpha), \quad x \in \mathbb{R}^3, \alpha \in \mathbb{R}, \quad (7.18)$$

that has for all  $\alpha$  with sufficiently small  $|\alpha|$  an equilibrium  $x_0 = 0$  with two complex eigenvalues  $\lambda_{1,2}(\alpha) = \mu(\alpha) \pm i\omega(\alpha)$  such that  $\mu(0) < 0, \omega(0) > 0$ , and one real eigenvalue  $\lambda_3(\alpha) = \gamma(\alpha)$  with  $\gamma(0) > 0$ . Suppose that at  $\alpha = 0$  the system has an orbit  $\Gamma_0$  homoclinic to  $x_0$ .

(i) If  $\mu(0) + \gamma(0) > 0$  then for all  $\alpha$  with sufficiently small  $|\alpha|$ , system (7.18) has an infinite number of saddle limit cycles in a neighborhood of  $\Gamma_0 \cup x_0$ .

(ii) If  $\mu(0) + \gamma(0) < 0$  then, generically, a hyperbolic stable limit cycle appears in a neighbourhood of  $\Gamma_0 \cup x_0$  for  $\alpha > 0$  or  $\alpha < 0$  with sufficiently small  $|\alpha|$ , while no other limit cycle exists in this neighbourhood for all  $\alpha$  with sufficiently small  $|\alpha|$ .

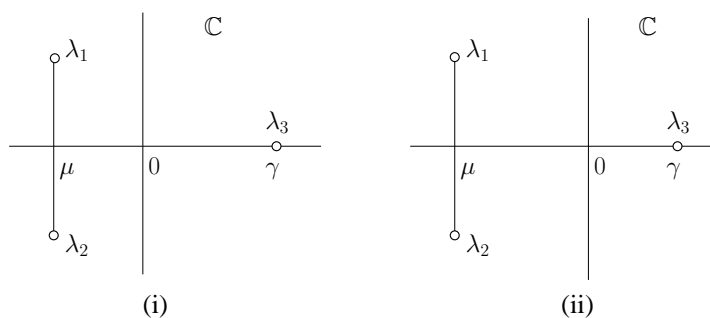


Figure 7.15: Eigenvalues of a saddle-focus.

**Remark:** An equilibrium  $x_0$  of (7.18) with a pair of complex-conjugate eigenvalues and a real eigenvalue is called a *saddle-focus*. The real number

$$\sigma_0 = \mu(0) + \gamma(0) = \operatorname{Re} \lambda_{1,2}(0) + \lambda_3(0)$$

is called the *saddle quantity* of  $x_0$ . In case (i), when  $\sigma_0 > 0$ , the two complex-conjugate eigenvalues  $\lambda_{1,2}$  are closer to the imaginary axis than the real positive eigenvalue  $\lambda_3$ , see Figure 7.15(i). In case (ii), when  $\sigma_0 < 0$ , the real positive eigenvalue  $\lambda_3$  is closer to the imaginary axis than the two complex-conjugate eigenvalues  $\lambda_{1,2}$ , see Figure 7.15(ii). An eigenvalue with the minimal  $|\operatorname{Re}\lambda|$  is called *determining*. Thus, each determining eigenvalue is complex in case (i) but real in case (ii).  $\diamond$

**Sketch of the proof:**

*Step 1 (Local straightening of invariant manifolds).* Write system (7.18) in a basis, where its linear part assumes the real canonical form, i.e.

$$\begin{cases} \dot{x}_1 &= \mu(\alpha)x_1 - \omega(\alpha)x_2 + F_1(x_1, x_2, x_3, \alpha), \\ \dot{x}_2 &= \omega(\alpha)x_1 + \mu(\alpha)x_2 + F_2(x_1, x_2, x_3, \alpha), \\ \dot{x}_3 &= \gamma(\alpha)x_3 + F_3(x_1, x_2, x_3, \alpha), \end{cases} \quad (7.19)$$

where  $F_k(x, \alpha) = O(\|x\|^2)$ ,  $k = 1, 2, 3$ , are smooth functions. According to Theorem 6.1, there exist stable and unstable parameter-dependent invariant manifolds of  $x_0$  which can be represented locally as

$$W_{\text{loc}}^u(0) = \{x \in \mathbb{R}^3 : x_1 = U_1(x_3, \alpha), x_2 = U_2(x_3, \alpha), |x_3| \leq d\}$$

and

$$W_{\text{loc}}^s(0) = \{x \in \mathbb{R}^3 : x_3 = V(x_1, x_2, \alpha), x_1^2 + x_2^2 \leq d^2\},$$

where  $d > 0$  is sufficiently small and the mappings  $U_{1,2} : \mathbb{R} \times \mathbb{R} \rightarrow \mathbb{R}^2$  and  $V : \mathbb{R}^2 \times \mathbb{R} \rightarrow \mathbb{R}$  are smooth, satisfy  $U_{1,2}(0, 0) = 0$  and  $V(0, 0) = 0$  and have vanishing first-order partial derivatives with respect to the  $x$ -variables at  $(x, \alpha) = (0, 0)$ . We shall assume that the homoclinic orbit corresponds to the part of  $W_{\text{loc}}^u(0)$  with  $x_3 > 0$ .

Introduce new coordinates  $(u_1, u_2, u_3)$  in  $\mathbb{R}^3$  by

$$\begin{cases} u_1 &= x_1 - U_1(x_3, \alpha), \\ u_2 &= x_2 - U_2(x_3, \alpha), \\ u_3 &= x_3 - V(x_1, x_2, \alpha). \end{cases} \quad (7.20)$$

In the  $u$ -coordinate system the stable manifold  $W^s(0)$  is (locally) the plane  $u_3 = 0$ , while  $W^u(0)$  is (also locally) the line  $u_1 = u_2 = 0$ . In these coordinates, the system (7.19) takes the form

$$\begin{cases} \dot{u}_1 &= \mu(\alpha)u_1 - \omega(\alpha)u_2 + P_1(u_1, u_2, u_3, \alpha), \\ \dot{u}_2 &= \omega(\alpha)u_1 + \mu(\alpha)u_2 + P_2(u_1, u_2, u_3, \alpha), \\ \dot{u}_3 &= \gamma(\alpha)u_3 + P_3(u_1, u_2, u_3, \alpha), \end{cases} \quad (7.21)$$

with smooth<sup>1</sup> functions  $P_k(u, \alpha) = O(\|u\|^2)$ ,  $k = 1, 2, 3$ , satisfying for small  $\|u\|$  and  $|\alpha|$

$$P_1(0, 0, u_3, \alpha) = P_2(0, 0, u_3, \alpha) = 0, \quad P_3(u_1, u_2, 0, \alpha) = 0.$$

---

<sup>1</sup>If the system (7.19) is  $C^r$ -smooth, the resulting system (7.21) is only  $C^{r-1}$ -smooth in general. Indeed, the mappings  $U$  and  $V$  are  $C^r$ -smooth, but we differentiate them once while transforming (7.19) into (7.21) using (7.20).

*Step 2 (Time reparametrization).* Since

$$\gamma(\alpha)u_3 + P_3(u_1, u_2, u_3, \alpha) = \gamma(\alpha)u_3(1 + R_3(u_1, u_2, u_3, \alpha)),$$

where  $R_3(u, \alpha) = O(\|u\|)$ , we can parametrize orbits of (7.21) near the origin by the new time  $\tau$  with

$$d\tau = (1 + R_3(u, \alpha)) dt$$

and consider a system that is locally orbitally equivalent to (7.21), namely:

$$\begin{cases} \dot{u}_1 &= \mu(\alpha)u_1 - \omega(\alpha)u_2 + Q_1(u_1, u_2, u_3, \alpha), \\ \dot{u}_2 &= \omega(\alpha)u_1 + \mu(\alpha)u_2 + Q_2(u_1, u_2, u_3, \alpha), \\ \dot{u}_3 &= \gamma(\alpha)u_3, \end{cases} \quad (7.22)$$

where the functions  $Q_j(u, \alpha) = O(\|u\|^2)$  are smooth and satisfy

$$Q_1(0, 0, u_3, \alpha) = Q_2(0, 0, u_3, \alpha) = 0$$

for small  $\|u\|$  and  $|\alpha|$ .

*Step 3 (Local  $C^1$ -linearization of system (7.22)).* The flow generated by system (7.22) is locally  $C^1$ -conjugate near the origin to the flow

$$\begin{pmatrix} \xi_1 \\ \xi_2 \\ \xi_3 \end{pmatrix} \mapsto \begin{pmatrix} e^{\mu(\alpha)\tau}[\xi_1 \cos(\omega(\alpha)\tau) - \xi_2 \sin(\omega(\alpha)\tau)] \\ e^{\mu(\alpha)\tau}[\xi_1 \sin(\omega(\alpha)\tau) + \xi_2 \cos(\omega(\alpha)\tau)] \\ \xi_3 e^{\gamma(\alpha)\tau} \end{pmatrix} \quad (7.23)$$

of its linearization

$$\begin{cases} \dot{\xi}_1 &= \mu(\alpha)\xi_1 - \omega(\alpha)\xi_2, \\ \dot{\xi}_2 &= \omega(\alpha)\xi_1 + \mu(\alpha)\xi_2, \\ \dot{\xi}_3 &= \gamma(\alpha)\xi_3. \end{cases} \quad (7.24)$$

To construct a local conjugating map  $h : \mathbb{R}^3 \rightarrow \mathbb{R}^3$ ,  $\xi = h(u)$ , one can use the following geometric construction. Introduce new coordinates  $(r, \varphi, z)$  in the  $u$ -space by

$$\begin{cases} u_1 &= r \cos \varphi, \\ u_2 &= r \sin \varphi, \\ u_3 &= z, \end{cases}$$

and consider a finite cylinder

$$\Omega = \{(r, \varphi, z) : 0 \leq r \leq d, |z| \leq d\}$$

with sufficiently small  $d > 0$  (see Figure 7.16(a)).

Take a point  $u \in \Omega$  that does not belong to the  $u_3$ -axis and consider the orbit of (7.22) arriving to this point at  $\tau = 0$ . Provided  $d$  is small enough, it can be shown that there is a smooth function  $\tau^0 = \tau^0(u, \alpha) < 0$  such that for  $\tau = \tau^0$  this orbit passes through the boundary  $r = d$  of  $\Omega$  at some point

$$u^0 = (d \cos \varphi^0(u, \alpha), d \sin \varphi^0(u, \alpha), z^0(u, \alpha)) \in \partial\Omega,$$

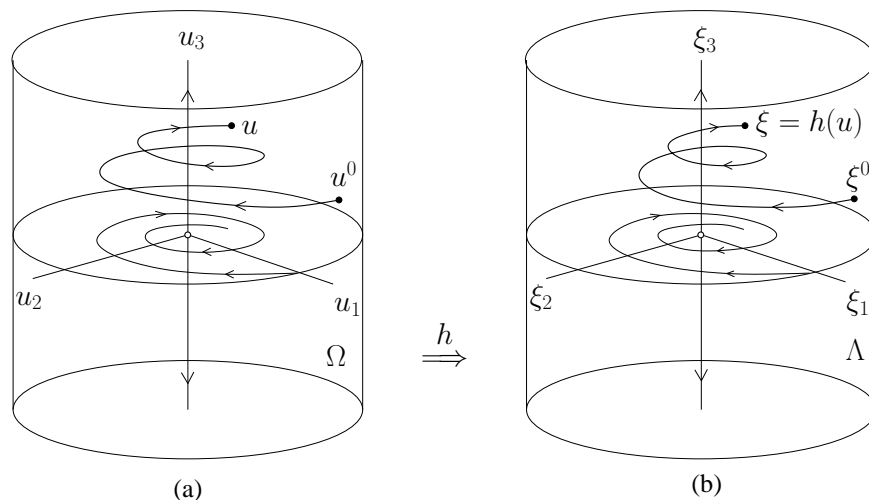


Figure 7.16: Local linearization of the system near a saddle-focus.

where

$$z^0(u, \alpha) = ze^{\gamma(\alpha)\tau^0(u, \alpha)}.$$

Also introduce the coordinates  $(\rho, \psi, \zeta)$  in the  $\xi$ -space by

$$\begin{cases} \xi_1 = \rho \cos \psi, \\ \xi_2 = \rho \sin \psi, \\ \xi_3 = \zeta, \end{cases}$$

and consider the cylinder

$$\Lambda = \{(\rho, \psi, \zeta) : 0 \leq \rho \leq d, |\zeta| \leq d\}$$

with the same  $d$  as before (see Figure 7.16(b)). Map the point  $u^0$  to the point

$$\xi^0 = (d \cos \varphi^0(u, \alpha), d \sin \varphi^0(u, \alpha), z^0(u, \alpha)) \in \partial\Lambda$$

and construct an orbit of the linear system (7.24) starting at  $\xi^0$ . The point  $\xi = h(u)$  is by definition the image of  $\xi^0$  under the flow (7.23) with  $\tau = -\tau^0(u, \alpha) > 0$ , i.e.

$$\begin{pmatrix} \xi_1 \\ \xi_2 \\ \xi_3 \end{pmatrix} = \begin{pmatrix} d e^{-\mu\tau^0(u, \alpha)} \cos [\varphi^0(u, \alpha) - \omega(\alpha)\tau^0(u, \alpha)] \\ d e^{-\mu\tau^0(u, \alpha)} \sin [\varphi^0(u, \alpha) - \omega(\alpha)\tau^0(u, \alpha)] \\ u_3 \end{pmatrix}. \quad (7.25)$$

Let  $h$  map the  $z$ -axis into itself according to the identity, i.e.  $\xi_3 = u_3$ . The resulting map  $u \mapsto \xi = h(u)$  is a local homeomorphism  $h : \Omega \rightarrow \Lambda$ . It obviously sends orbits of (7.22) into orbits of the linear system (7.24), preserving time parametrization. By construction, it is smooth away from the  $z$ -axis. It can be shown that  $h$  also has continuous first-order partial derivatives at points on the  $z$ -axis in  $\Lambda$ . In general, higher-order derivatives are not continuous but the  $C^1$ -smoothness of  $h$  is sufficient for our purposes. We can also extend the constructed map to a globally defined  $C^1$ -diffeomorphism  $h : \mathbb{R}^3 \rightarrow \mathbb{R}^3$  that locally conjugates the flows of (7.22) and (7.24). We will use the  $(\rho, \psi, \zeta)$ -coordinates in the following analysis.



Therefore, the map  $\Delta$  can be explicitly computed for all sufficiently small  $|\alpha|$  as  $\Delta(\psi, \zeta) = \xi$  where

$$\Delta : \begin{cases} \xi_1 &= d \left( \frac{\zeta}{d} \right)^{q(\alpha)} \cos \left( \psi - \frac{\omega(\alpha)}{\gamma(\alpha)} \ln \frac{\zeta}{d} \right), \\ \xi_2 &= d \left( \frac{\zeta}{d} \right)^{q(\alpha)} \sin \left( \psi - \frac{\omega(\alpha)}{\gamma(\alpha)} \ln \frac{\zeta}{d} \right), \end{cases} \quad (7.26)$$

where

$$q(\alpha) = -\frac{\mu(\alpha)}{\gamma(\alpha)} > 0. \quad (7.27)$$

It follows from (7.26) that the image  $\Delta\Sigma^+$  of  $\Sigma^+$  is a “solid spiral” in  $H$  as shown in Figure 7.17. It is contained in the disc

$$\Pi = \left\{ (\xi_1, \xi_2) : 0 \leq \rho \leq d \left( \frac{\varepsilon}{d} \right)^{q(\alpha)} \right\} \subset H.$$

The global map  $\mathcal{Q}$  is a  $C^1$ -diffeomorphism that maps  $\Pi$  back to  $S$ . We can write this map as

$$\mathcal{Q} : \begin{cases} \psi &= \nu(\alpha) + a_{11}(\alpha)\xi_1 + a_{12}(\alpha)\xi_2 + o(\rho), \\ \zeta &= \beta(\alpha) + a_{21}(\alpha)\xi_1 + a_{22}(\alpha)\xi_2 + o(\rho), \end{cases} \quad (7.28)$$

where  $\nu(0) = \beta(0) = 0$  but  $a_{11}(0)a_{22}(0) - a_{21}(0)a_{12}(0) \neq 0$ . The function  $\beta = \beta(\alpha)$  gives the relative  $\zeta$ -displacement of the invariant manifolds  $W^s(x_0)$  and  $W^u(x_0)$  for small  $\alpha \neq 0$ . Generically  $\beta'(0) \neq 0$ , so its value can be considered as a new bifurcation parameter. The image  $\mathcal{Q}\Pi$  is a deformed disc with the  $O(\varepsilon^{q(\alpha)})$ -height in the  $\zeta$ -direction for  $\varepsilon \rightarrow 0$ .

If  $\varepsilon$  is sufficiently small, the composition  $\mathcal{Q} \circ \Delta$  defines the Poincaré map  $\mathcal{P} : \Sigma^+ \rightarrow S$  that can be written using (7.26) and (7.28) as

$$\mathcal{P} : \begin{cases} \psi &= \nu(\alpha) + A(\alpha)d \left( \frac{\zeta}{d} \right)^{q(\alpha)} \cos \left( \psi - \frac{\omega(\alpha)}{\gamma(\alpha)} \ln \frac{\zeta}{d} + \psi_1(\alpha) \right) + o(\zeta^{q(\alpha)}), \\ \zeta &= \beta(\alpha) + B(\alpha)d \left( \frac{\zeta}{d} \right)^{q(\alpha)} \cos \left( \psi - \frac{\omega(\alpha)}{\gamma(\alpha)} \ln \frac{\zeta}{d} + \psi_2(\alpha) \right) + o(\zeta^{q(\alpha)}), \end{cases} \quad (7.29)$$

for  $\zeta \rightarrow 0$ , where  $A(\alpha), B(\alpha), \psi_j(\alpha)$  are smooth functions determined by  $a_{kl}(\alpha)$  and  $q(\alpha)$ .

*Step 6 (Analysis of the Poincaré map at  $\alpha = 0$ ).* It is clear that no periodic orbit can start in  $\Sigma^-$ . Therefore, consider the intersection of the spiral image  $\mathcal{P}\Sigma^+$  with  $\Sigma$  (see Figure 7.18). The origin of the image is at the intersection of  $\Gamma_0$  with  $\Sigma$ , i.e. at the point  $(\rho, \psi, \zeta) = (d, 0, 0)$ . The intersection of  $\Sigma$  with  $W^s(x_0)$  corresponding to  $\zeta = 0$  splits the spiral into an infinite number of *upper* and *lower* “half-turns.” The preimages  $\Sigma_j$  of the upper “half-turns”  $\mathcal{P}\Sigma_j$ ,  $j = 1, 2, \dots$ , are almost horizontal strips in  $\Sigma^+$ , which are located between the lines

$$\zeta = \zeta_k = C(0)e^{-\pi k \gamma(0)/\omega(0)}(1 + o(1)), \quad k \rightarrow \infty, \quad (7.30)$$

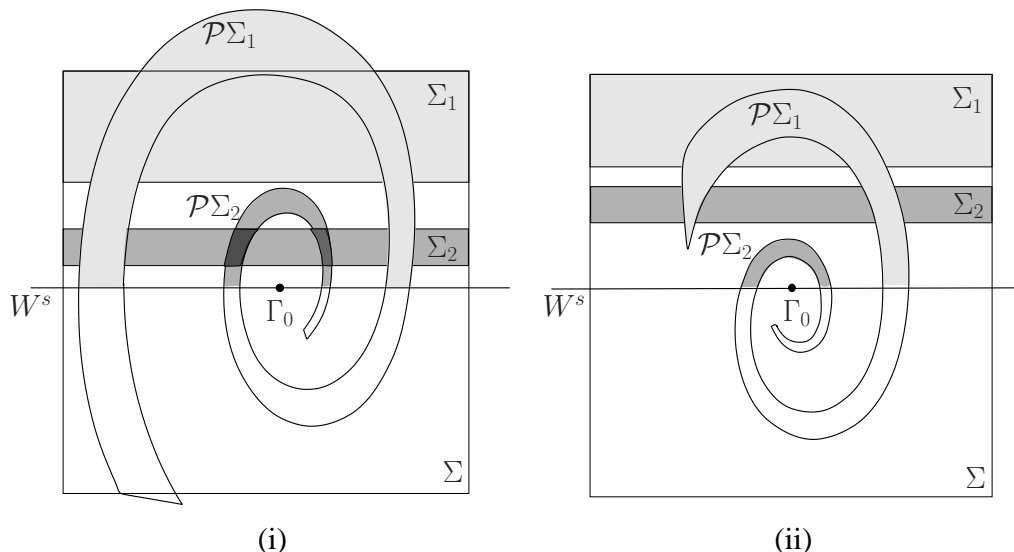


Figure 7.18: Case  $\alpha = 0$ : (i)  $q(0) < 1$ , i.e.  $\sigma_0 > 0$ ; (ii)  $q(0) > 1$ , i.e.  $\sigma_0 < 0$ .

corresponding to  $k = 2j$  and  $k = 2j + 1$  (see (7.29)). Here  $C(\alpha)$  is a smooth function. These strips accumulate on  $\zeta = 0$  as  $k \rightarrow \infty$ . As follows from (7.30) and (7.29), the  $\zeta$ -coordinate of the top of the  $j$ -th half-spiral is estimated by

$$\zeta_{2j}^{q(0)} = O\left(e^{-2\pi j \mu(0)/\omega(0)}\right), \quad j \rightarrow \infty.$$

Then we can distinguish two cases (see Figure 7.18):

(i) If  $\mu(0) + \gamma(0) > 0$  then  $q(0) < 1$ . Therefore, the intersection  $\Sigma_j \cap \mathcal{P}\Sigma_j$  is nonempty and consists of two components for  $j \geq j_0$ , where  $j_0$  is an integer number ( $j_0 = 2$  in Figure 7.18(i)). Hence, each intersection with sufficiently big index  $j$  forms a Smale Horseshoe to which Theorem 7.36 applies. Each horseshoe implies an infinite number of saddle cycles. These cycles of  $\mathcal{P}$  correspond to saddle limit cycles of (7.18).

(ii) If  $\mu(0) + \gamma(0) < 0$  then  $q(0) > 1$ . Therefore, there is some index  $j_0 > 0$  such that for  $j \geq j_0$  the intersection  $\Sigma_j \cap \mathcal{P}\Sigma_j$  is empty for  $\alpha = 0$  ( $j_0 = 2$  in Figure 7.18(ii)). Thus, there are no fixed points (or cycles) of  $\mathcal{P}$  in  $\Sigma^+$  close to  $\Gamma_0$ .

*Step 7 (Analysis of the Poincaré map for small  $|\alpha| \neq 0$ ).* If  $\alpha \neq 0$ , the point corresponding to the intersection of the unstable manifold of  $x_0$  with  $S$  is generically displaced from the horizontal line  $\zeta = 0$  in  $\Sigma$  and becomes  $(\rho, \psi, \zeta) = (d, \nu(\alpha), \beta(\alpha))$  with  $\beta \neq 0$ . Also in this situation, no periodic orbit can start in  $\Sigma^-$ .

In case (i), there remains in general only a *finite* number of Smale Horseshoes of  $\mathcal{P}$  for small  $|\beta(\alpha)|$ . They still generate an infinite number of saddle limit cycles in (7.18) for all  $\alpha$  with sufficiently small  $|\alpha|$ .

In case (ii), the map  $\mathcal{P}$  is a contraction in  $\Sigma^+$  for  $\beta(\alpha) > 0$  and thus has a unique attracting fixed point corresponding to a stable limit cycle of (7.18). There are no other periodic orbits nearby. For small fixed  $\beta(\alpha) < 0$ , there is  $h > 0$  such that  $\Sigma^+ \cap \mathcal{P}\Sigma^+ = \emptyset$ , implying that no periodic orbits can exist in  $\Sigma^+$  for small  $\beta(\alpha) < 0$ .

□

**Remark:** Fine bifurcation details in case (i) depend on another saddle quantity

$$\sigma_1 = 2\mu(0) + \gamma(0) = 2\operatorname{Re} \lambda_{1,2}(0) + \lambda_3(0) = \operatorname{div} f(0, 0).$$

If  $\sigma_1 < 0$  then for a countable number of parameter intervals the system (7.18) has a *stable cycle*. If  $\sigma_1 > 0$  then for a countable number of parameter intervals the system (7.18) has a *repelling cycle*.  $\diamond$

**Example 7.40 (Homoclinic orbits to saddle-foci in Arneodo's system)**

Both cases of Theorem 7.39 can be illustrated using the system<sup>2</sup>

$$\begin{cases} \dot{x}_1 = x_2, \\ \dot{x}_2 = x_3, \\ \dot{x}_3 = -x_3 - bx_2 + cx_1 - x_1^2, \end{cases} \quad (7.31)$$

that appears in the analysis of bifurcations of an equilibrium with triple-zero eigenvalue. This system exhibits many homoclinic bifurcations.

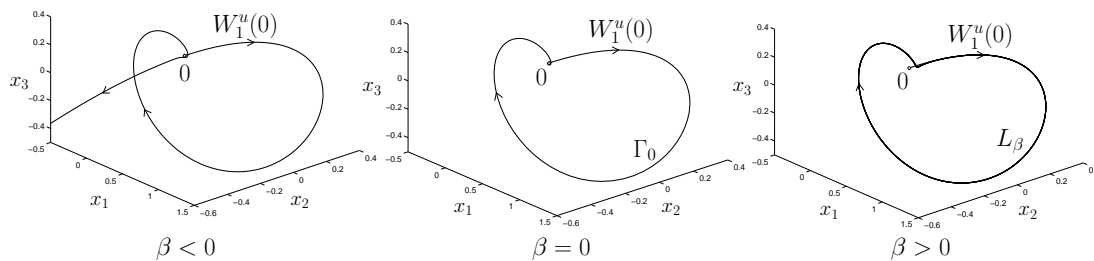


Figure 7.19: The unstable invariant manifold  $W_1^u(0)$  of the saddle-focus near a homoclinic bifurcation in (7.31) when  $\mu(0) + \gamma(0) < 0$ .

If  $b = 0.5$  then at  $c = 0.964149\dots$  the system (7.31) has a homoclinic orbit  $\Gamma_0$  to the saddle-focus equilibrium  $x_0 = 0$ . Since the eigenvalues of the corresponding Jacobian matrix

$$\begin{pmatrix} 0 & 1 & 0 \\ 0 & 0 & 1 \\ c & -b & -1 \end{pmatrix}$$

are

$$\lambda_{1,2} = -0.81537\dots \pm i0.92938\dots, \quad \lambda_3 = 0.6307\dots,$$

case (ii) applies. Thus, a unique and stable limit cycle bifurcates from  $\Gamma_0$  for  $\beta > 0$  (see Figure 7.19). A branch  $W_1^u(0)$  of the unstable invariant manifold of the saddle-focus tends to this cycle when it exists. This phenomenon can easily be seen by numerically integrating (7.31). The left picture in Figure 7.19 corresponds to the parameter value  $c = 0.960$ , while for the right one the value  $c = 0.965$  is used.

<sup>2</sup>Arneodo, A., Coulet, P.H., Spiegel, E.A., and Tresser, C. 'Asymptotic chaos', *Physica D* **14** (1985), 327-347.

If  $c = 5$  then at  $b = 1.870532\dots$  the system (7.31) also has a homoclinic orbit  $\Gamma_0$  to the saddle-focus equilibrium  $x_0$  at the origin. Here the eigenvalues of the corresponding Jacobian matrix are

$$\lambda_{1,2} = -1.0753\dots \pm i1.78575\dots, \quad \lambda_3 = 1.150677\dots,$$

so we are in case (i). Thus, infinitely-many saddle limit cycles ought to exist near  $\Gamma_0$  for all  $\alpha$  with sufficiently small  $|\alpha|$ . Since  $\sigma_1 < 0$ , infinitely-many parameter intervals exist for  $\beta > 0$ , where (7.31) also has a stable cycle. This cycle, however, is hardly observable in numerical simulations, since its domain of attraction is very small.

As in the previous case,  $W_1^u(0)$  leaves the neighbourhood of  $\Gamma_0$  for  $\beta < 0$ . For small  $\beta > 0$ ,  $W_1^u(0)$  can either remain in this neighbourhood indefinitely (e.g., approaching one of the cycles) or leave it after a number of turns near  $\Gamma_0$ . The left and the right pictures in Figure 7.20 correspond to  $b = 1.870$  and  $b = 1.875$ , respectively.

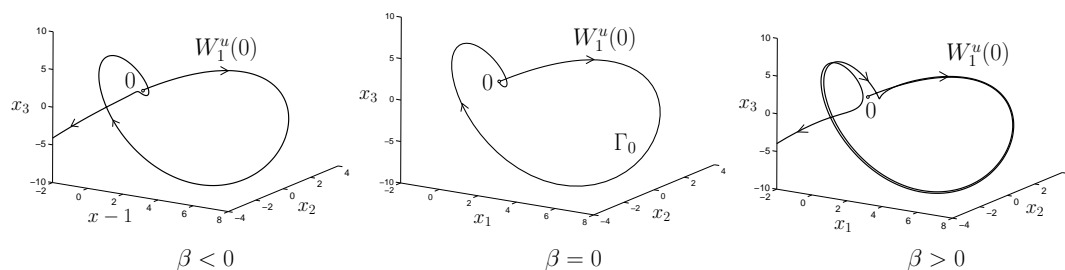


Figure 7.20: The unstable invariant manifold  $W_1^u(0)$  of the saddle-focus near a homoclinic bifurcation in (7.31) when  $\mu(0) + \gamma(0) > 0$ :

#### Example 7.41 (Homoclinic chaos in Rössler's system)

A homoclinic orbit to a saddle-focus, with an infinite number of saddle cycles nearby, can be embedded in a larger attracting set, thus generating stable chaotic motions. A famous example of this phenomenon is provided by *Rössler's prototype chaotic system*<sup>3</sup>

$$\begin{cases} \dot{x}_1 = -x_2 - x_3, \\ \dot{x}_2 = x_1 + Ax_2, \\ \dot{x}_3 = Bx_1 - Cx_3 + x_1x_3, \end{cases} \quad (7.32)$$

with fixed  $A = 0.36$  and  $C = 0.4$ . For these parameter values, (7.32) has an orbit  $\Gamma_0$  homoclinic to the saddle-focus equilibrium  $x_0 = (0, 0, 0)$  at  $B = 0.370322\dots$ . This equilibrium has eigenvalues

$$\lambda_{1,2} = 0.085618\dots \pm i1.12034\dots, \quad \lambda_3 = -0.211236\dots,$$

<sup>3</sup>Rössler, O.E. 'Continuous chaos—four prototype equations', In: Bifurcation Theory and Applications in Scientific Disciplines, *Ann. New York Acad. Sci.* **316**, New York, 1979, pp. 376–392.

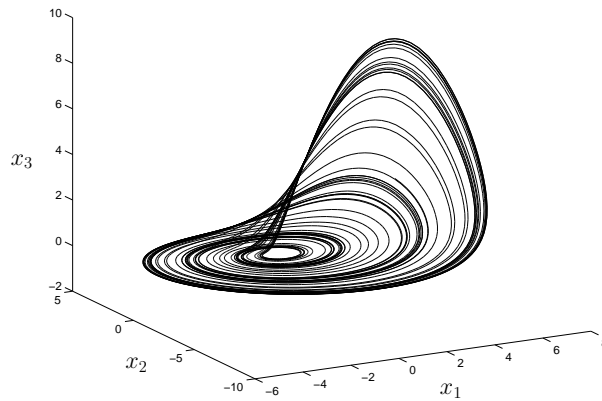


Figure 7.21: Shilnikov chaos near a homoclinic orbit to a saddle-focus.

so that one has to reverse time to apply Theorem 7.39. After that, we are evidently in case (i). A direct numerical integration of (7.32) with generic initial data reveals stable nonperiodic behaviour that persists for nearby values of the parameter  $B$  (see Figure 7.21 corresponding to  $B = 0.4$ ). Note that long-periodic stable cycles are also present here but hardly observable numerically.

## 7.3 References

This chapter is a brief introduction to “chaotic dynamics” and global bifurcations. More extensive introductions are [Katok & Hasselblatt 1995, Alligood et al. 1997, Hasselblatt & Katok 2003, Wiggins 2003].

The dynamics generated by one-dimensional maps is a classical mathematical subject, studied in details. It is included in many introductory texts on dynamical systems, e.g. [Guckenheimer & Holmes 1983, van Strien 1991, Verhulst 1996, Brin & Stuck 2002, Hasselblatt & Katok 2003]. Proofs of Sharkovsky’s Theorem can be found, for example, in [Devaney 1989, Katok & Hasselblatt 1995, Brin & Stuck 2002]. The Feigenbaum universality in period-doubling cascades is discussed in [Coullet & Eckmann 1980, Guckenheimer & Holmes 1983, Lyubich 2000].

The Smale Horseshoe is treated in the classical books [Nitecki 1971, Moser 1973], as well as in all textbooks mentioned above. A nice color representation of the horseshoe is given in [Shub 2005].

The complicated structure formed by the intersecting invariant manifolds near a homoclinic orbit to a saddle fixed point has been discovered by Poincaré in 1890’s. It is treated, together with Shilnikov’s phenomena near a homoclinic orbit to a saddle-focus, in [Guckenheimer & Holmes 1983, Wiggins 1988, Wiggins 2003, Kuznetsov 2004]. The theory of homoclinic bifurcations is systematically presented in [Arnol’d et al. 1994, Ilyashenko & Li 1999] and, in particular, in [Shilnikov et al. 1998, Shilnikov et al. 2001]. For an account of analytical and numerical results on Lorenz system, see [Viana 2000].

Numerical methods for bifurcations of homoclinic orbits to equilibria in ODEs are summarized in [Beyn et al. 2002].

## 7.4 Exercises

### E 7.4.1 (Smale Horseshoe in Hénon map)

Consider the following planar quadratic map depending on two parameters:

$$f_{(\alpha,\beta)} : \begin{pmatrix} x \\ y \end{pmatrix} \mapsto \begin{pmatrix} x \\ \alpha - \beta x - y^2 \end{pmatrix}. \quad (7.33)$$

An equivalent map was introduced by Hénon<sup>4</sup> as the simplest map with “chaotic behaviour.”

1. Prove that  $f_{(\alpha,\beta)}$  is invertible if  $\beta \neq 0$ .
2. Find a horseshoe for map (7.33) at  $(\alpha, \beta) = (4.5, 0.2)$ . (*Hint:* Consider the image  $f_{(\alpha,\beta)}(R)$  of a rectangle  $R$  shown in Figure 7.22.)

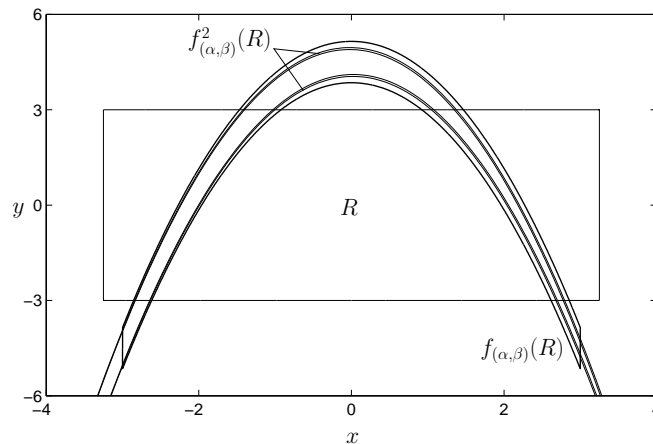


Figure 7.22: Smale horseshoe in the Hénon map.

### E 7.4.2 (Schwarzian derivative)

**Definition 7.42** The *Schwarzian derivative* of a smooth function  $f : \mathbb{R} \rightarrow \mathbb{R}$  at  $x$  is

$$(Sf)(x) = \frac{f'''(x)}{f'(x)} - \frac{3}{2} \left( \frac{f''(x)}{f'(x)} \right)^2.$$

We will write  $Sf < 0$  if for all  $x \in \mathbb{R}$  either  $(Sf)(x) < 0$  or  $\lim_{\xi \rightarrow x} (Sf)(\xi) = -\infty$ . Prove the following statements:

1. Let  $P(x)$  be a polynomial such that all roots of  $P'(x)$  are real and distinct. Then  $SP < 0$ .
2. Suppose that  $Sf < 0$  and  $f$  has  $n$  critical points. Then  $f$  has at most  $n + 2$  attracting periodic orbits.

<sup>4</sup>Hénon, M. ‘A two-dimensional mapping with a strange attractor’, *J Comm. Math. Phys.* **50** (1976), 69-77.

3. Let  $Sf < 0$  and  $Sg < 0$ . Then holds  $S(f \circ g) < 0$ .
4. Only supercritical period-doubling bifurcations of fixed points and cycles can occur in a family of smooth functions  $f_{(\alpha)} : \mathbb{R} \rightarrow \mathbb{R}$  with  $Sf_{(\alpha)} < 0$ . (*Hint*: Use the formula (5.61) for the critical normal form coefficient  $c$  at the period-doubling bifurcation.)

### E 7.4.3 (Travelling pulses in the FitzHugh-Nagumo model)

The following system of partial differential equations is the FitzHugh-Nagumo simplification<sup>5</sup> of the Hodgkin-Huxley PDEs describing the nerve impulse propagation along an axon:

$$\begin{cases} \frac{\partial u}{\partial t} = \frac{\partial^2 u}{\partial x^2} - f_a(u) - v, \\ \frac{\partial v}{\partial t} = bu, \end{cases} \quad (7.34)$$

where  $u = u(x, t)$  represents the membrane potential,  $v = v(x, t)$  is a “recovery” variable,  $f_a(u) = u(u - a)(u - 1)$ ,  $1 > a > 0$ ,  $b > 0$ ,  $-\infty < x < +\infty$ , and  $t > 0$ .

*Traveling waves* are solutions to these equations of the form

$$u(x, t) = U(\xi), \quad v(x, t) = V(\xi), \quad \xi = x + ct,$$

where  $c > 0$  is an a priori unknown wave propagation speed.

1. Verify that  $U(\xi)$  and  $V(\xi)$  satisfy the following system of three autonomous ODEs:

$$\begin{cases} \dot{U} = W, \\ \dot{W} = cW + f_a(U) + V, \\ \dot{V} = \frac{b}{c}U, \end{cases} \quad (7.35)$$

where the dot means differentiation with respect to “time”  $\xi$ . System (7.35) is called the *wave system* for (7.34); it depends on three positive parameters  $(a, b, c)$ .

2. Check that for all  $c > 0$  the wave system (7.35) has a unique equilibrium  $O$  with one positive eigenvalue  $\lambda_3$  and two eigenvalues  $\lambda_{1,2}$  with negative real parts. Conclude that this equilibrium has a one-dimensional unstable invariant manifold and a two-dimensional stable invariant manifold.
3. Show that for fixed  $b > 0$  the eigenvalues  $\lambda_{1,2}$  can either be real or form a complex-conjugate pair. Find a condition on the system parameters that defines a boundary between these two cases. Plot the boundaries in the  $(a, c)$ -plane corresponding to  $b = 0.01, 0.005, 0.0025$ , and specify in each case the region corresponding to saddle-foci. (*Hint*: At the curve

$$D_b = \{(a, c) : c^4(4b - a^2) + 2ac^2(9b - 2a^2) + 27b^2 = 0\}.$$

the characteristic polynomial  $h(\lambda)$  has a double root  $\lambda_0$  satisfying  $h(\lambda_0) = h'(\lambda_0) = 0$ .)

4. A *travelling pulse* corresponds to a homoclinic orbit to  $O$  of (7.35), along which

$$(U(\xi), V(\xi), W(\xi)) \rightarrow (0, 0, 0)$$

as  $\xi \rightarrow \pm\infty$ . Sketch possible profiles of traveling pulses in both regions. (*Hint*: See Figure 7.23.)

5. Show that the saddle quantity  $\sigma_0$  of the equilibrium  $O$  in the wave system (7.35) is positive. (*Hint*:  $\lambda_1 + \lambda_2 + \lambda_3 = c > 0$ .)

---

<sup>5</sup>FitzHugh, R. ‘Impulses and physiological states in theoretical models of nerve membrane’, *Biophys. J.* **1** (1961), 445-446; J. Nagumo, S. Arimoto, and S. Yoshizawa ‘An active pulse transmission line simulating nerve axon’, *Proc. IRE* **50** (1962), 2061-2070.

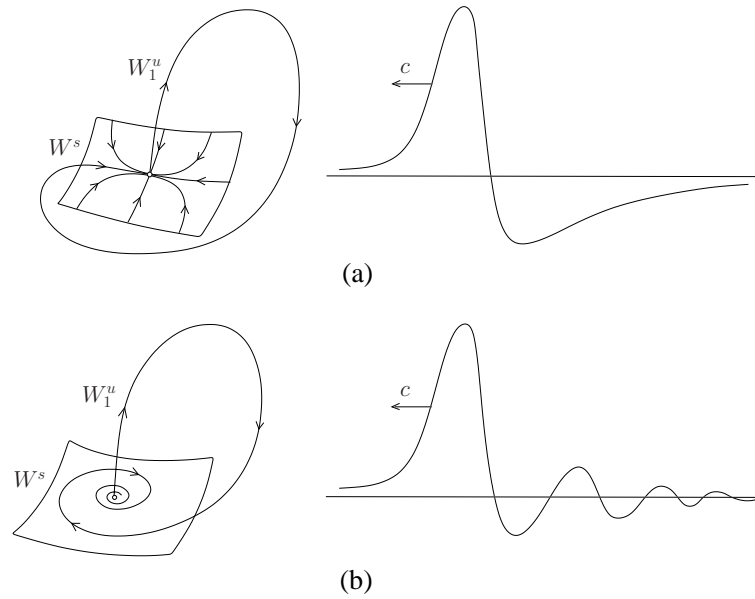


Figure 7.23: Pulses with monotone (a) and oscillating (b) “tails”.

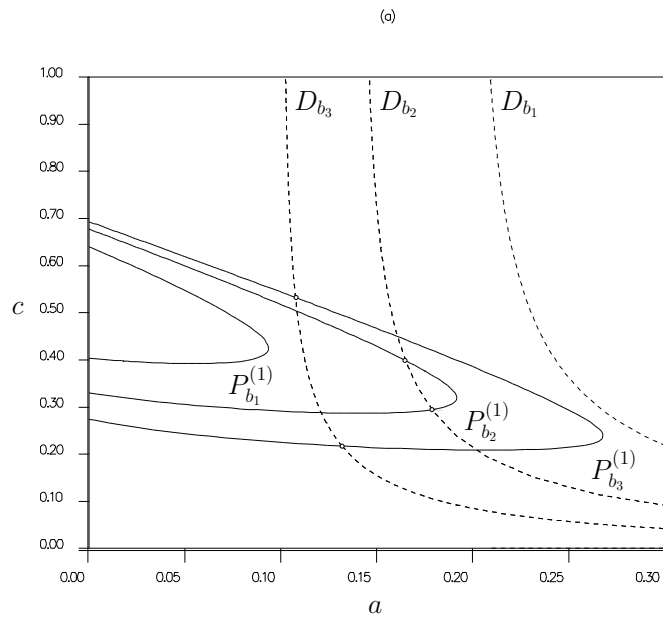


Figure 7.24: Bifurcation curves of the wave system (7.35) for  $b_1 = 0.01$ ,  $b_2 = 0.005$ , and  $b_3 = 0.0025$ .

6. Compute numerically curves  $P_b^{(1)}$  in the  $(a, c)$ -plane for  $b = 0.01, 0.005, 0.0025$ , which correspond to the existence of the simplest homoclinic orbit in (7.35) and verify that these bifurcation curves look like in Figure 7.24. (*Hint*: Use one of the standard software packages, e.g. HomCont<sup>6</sup> in AUTO97/2000/07P .)
7. Conclude that the computed bifurcation curves  $P_b^{(1)}$  pass through the saddle-focus region delimited by the corresponding curve  $D_b$ , and that for nearby parameter values the FitzHugh-Nagumo system (7.34) has infinitely many *periodic travelling waves*. (*Warning*: This analysis demonstrates the existence but says nothing about stability of these travelling waves as solutions to the PDE system (7.34).)

#### E 7.4.4 (Bounds for Lorenz attractor)

Let  $B_R$  be the closed ball of radius  $R$  centered at  $(0, 0, \sigma + r)$ . Prove that there exists  $R > 0$  such that

(i)  $B_R$  is positively invariant set for Lorenz system (7.56), see Appendix;

(ii) Every orbit of (7.56) enters  $B_R$ .

(*Hint*: Consider  $V(x, y, z) = x^2 + y^2 + z^2 - 2(\sigma + r)z$ . Choose  $\delta > 0$  and prove that for suitable  $M > 0$

$$\frac{d}{dt}V(x(t), y(t), z(t)) < -\delta,$$

provided  $V > M$ .)

#### E 7.4.5 (Homoclinic orbits in a slow-fast system in $\mathbb{R}^3$ )

1. Check that the following slow-fast system<sup>7</sup>

$$\begin{cases} \dot{x} &= (z + 1) + (1 - z)[(x - 1) - y], \\ \dot{y} &= (1 - z)[(x - 1) + y], \\ \varepsilon \dot{z} &= (1 - z^2)[z + 1 - m(x + 1)] - \varepsilon z, \end{cases} \quad (7.36)$$

has a homoclinic orbit to the equilibrium  $(1, 0, -1)$  in the *singular limit*  $\varepsilon = 0$ , provided  $m = 1$ . (*Hint*: Formally set  $\varepsilon = 0$  and analyze the equations on the *slow manifolds* defined by  $z = \pm 1$ .)

2. Determine the shape of the surface  $\dot{z} = 0$  for small  $\varepsilon > 0$ . Convince yourself that there exists a continuous function  $m = m(\varepsilon)$ ,  $m(0) = 1$ , defined for  $\varepsilon \geq 0$ , such that for the corresponding parameter value (7.36) has a saddle-focus with a homoclinic orbit.
3. Which case of Theorem 7.39 applies? How many periodic orbits one can expect near the bifurcation?

#### E 7.4.6 (Local birth of Lorenz attractor)

1. Rewrite the Lorenz system (7.56) introduced in Appendix using new variables  $(\xi, \eta, \zeta)$  such that

$$x = \sqrt{2}\xi, \quad y = \sqrt{2}\left(\xi + \frac{\eta}{\sigma}\right), \quad z = \frac{1}{\sigma}((2\sigma - b)\xi + \xi^2),$$

and assume that  $2\sigma \neq b$ . *Answer*: In the new variables the system will take the form:

$$\begin{cases} \dot{\xi} &= \eta, \\ \dot{\eta} &= \sigma(r - 1)\xi - (1 + \sigma)\eta - (2\sigma - b)\xi\zeta - \xi^3, \\ \dot{\zeta} &= -b\zeta + \xi^2. \end{cases}$$

<sup>6</sup>Champneys, A.R., Kuznetsov, Yu.A., and Sandstede, B. 'A numerical toolbox for homoclinic bifurcation analysis', *Internat. J. Bifur. Chaos* **6** (1996), 867-887.

<sup>7</sup>Deng, Bo 'Constructing homoclinic orbits and chaotic attractors', *Internat. J. Bifur. Chaos* **4** (1994), 823-841.

2. Introduce a small parameter  $\varepsilon > 0$  and set back

$$x(t) = \varepsilon \xi(\varepsilon t), \quad y(t) = \varepsilon^2 \eta(\varepsilon t), \quad z(t) = \varepsilon \zeta(\varepsilon t).$$

This yields

$$\begin{cases} \dot{x} &= y, \\ \dot{y} &= \varepsilon^2 \sigma(r-1)x - \varepsilon(1+\sigma)y - \varepsilon(2\sigma-b)xz - x^3, \\ \dot{z} &= -\varepsilon bz + x^2. \end{cases} \quad (7.37)$$

This allows us to consider (7.37) as a small perturbation of the singular system corresponding to  $\varepsilon = 0$ :

$$\begin{cases} \dot{x} &= y, \\ \dot{y} &= -x^3, \\ \dot{z} &= x^2, \end{cases} \quad (7.38)$$

having an equilibrium  $O = (0, 0, 0)$  with triple zero eigenvalue.

3. Let  $(\sigma, r, b)$  belong to the chaotic region for the original Lorenz system (7.56). Argue that (7.37) has a small but diffeomorphic strange attractor for small  $\varepsilon > 0$  which shrinks to  $O$  as  $\varepsilon \rightarrow 0$ .

#### E 7.4.7 (Linearization of the doubling operator)

Prove that the differential of the doubling operator (7.13) at its fixed point  $\varphi$  is given by the formula<sup>8</sup>

$$(\mathcal{L}(\varphi)h)(x) = \omega(x)h(1) - \frac{1}{\xi}[\varphi'(\varphi(\xi x))h(\xi x) + h(\varphi(\xi x))],$$

where  $\xi = -\varphi(1)$  and

$$\omega(x) = -\frac{1}{\xi^2}\varphi(\varphi(\xi x)) + \frac{1}{\xi}x\varphi'(\varphi(\xi x)).$$

---

<sup>8</sup>Petrovich, V. Yu. (1990) 'Numerical spectral analysis of the differential of the doubling operator by K.I. Babenko's method', Preprint 90-81, Institute of Applied Mathematics, USSR Academy of Sciences, Moscow. In Russian.